Analytical Methods

Accepted Manuscript

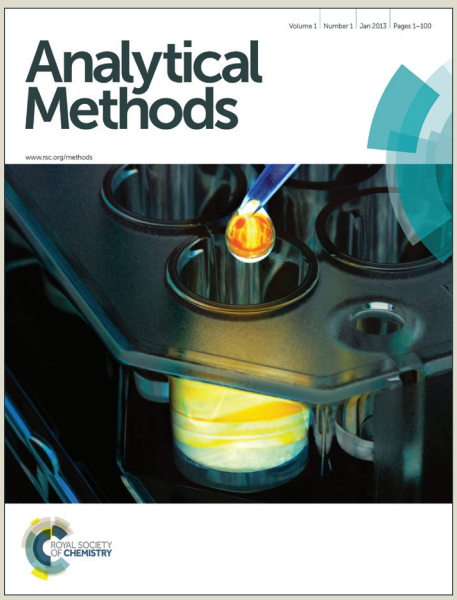

This is an *Accepted Manuscript*, which has been through the Royal Society of Chemistry peer review process and has been accepted for publication.

Accepted Manuscripts are published online shortly after acceptance, before technical editing, formatting and proof reading. Using this free service, authors can make their results available to the community, in citable form, before we publish the edited article. We will replace this *Accepted Manuscript* with the edited and formatted *Advance Article* as soon as it is available.

You can find more information about *Accepted Manuscripts* in the Information for Authors.

ROYAL SOCIETY OF CHEMISTRY

www.rsc.org/methods

Simple hydrothermal preparation of carbon nanodots and its colorimetric and fluorimetric detection of mercury ions

Yan Liang, Hui Zhang, Yan Zhang, Fang Chen*

Key Laboratory for Large-Format Battery Materials and System (Ministry of Education), School of Chemistry and Chemical Engineering, Huazhong University of Science and Technology, Wuhan 430074, P.R. China

Abstract

The present article reports on the one-step rapid green synthesis of water-soluble, fluorescent carbon nanodots (C-dots) with a quantum yield of 8.9%. Compared with previous hydrothermal method, the proposed method is performed at relatively lower temperature and results in larger size (20~30 nm) C-dots. We observes that UV-Vis absorbance at 302 nm of C-dots shows significant linear correlation with the concentration of Hg^{2+} added, which indicating that as-prepared carbon dots could act as a colorimetric probe of Hg^{2+}. Linear range of this colorimetric probe is 1.0×10^{-9}~7.0×10^{-7} mol L^{-1} and the detection limits is 5.7×10^{-10} mol L^{-1}. Simultaneously, fluorescence of the C-dots in pH 5.0 phosphate buffer solution can be dramatically quenched by Hg^{2+}, whereas nearly unaffected by other metal ions. A good linear

* Corresponding author: Tel.:+86-27-87543032, Fax:+86-27-87543632, E-mail: fchen@mail.hust.edu.cn

relation exists between the quenching efficiency (F_0/F) and the concentration of Hg^{2+} in the range of 7.0×10^{-9}~7.0×10^{-7} mol L^{-1} with a detection limit (3σ) of 5.5×10^{-10} mol L^{-1}. This dual probe of Hg^{2+} gives excellent performance in polluted tap water samples analysis, suggesting promising application in the future.

Keywords: Carbon nanodots, Colorimetry, Mercury ions, Fluorimetry,

1. Introduction

Mercury ion（Hg^{2+}）ranks top in the list of toxic heavy metal ions due to its deadly toxicity at low concentration as well as bio-accumulative effect in ecosystems.[1,2] Mercury ions, especially water-soluble Hg^{2+}, can easily pass through skin, respiratory and gastrointestinal tissues, leading to DNA damages, mitosis impairment and permanent damages to the central nervous system.[3] Therefore, urges to develop cheap, sensitive and rapid analytical method for the detection of trace amount of Hg^{2+} in aqueous system have persisted in the past few decades.[4] With the unremitting efforts made on this global problem over the years, different analytical methods have been developed. Beside the atomic absorption spectroscopy, cold vapor atomic fluorescence spectrometry and gas chromatography which requires expensive instrumentation and sophisticated sample preparation,[5] some methods based on organic chromophores [6] or fluorophores,[7,8] conjugated polymers,[9] gold nanoparticles,[10] Ag nanoclusters,[11] DNAzymes,[12] single-walled carbon

nanotubes,[13,14] nanogel,[15] aggregation induced emission (AIE) based fluorescence sensor[16], nano-C_{60}[17] and carbon dots[18,19]have raised great attention over the recent years. However, considering the complex and time-consuming synthesis routes, toxic or expensive reagents involved in methods above, developing a simple, sensitive and green analytical method for mercury ion detection is of high priority.

In the past several years, carbon dots (C-dots), or carbon nanoparticles (CPs), mainly consists of three kinds of fluorescent dots: grapheme quantum dots (GQDs), carbon nanodots (CNDs) and polymer dots (PDs).[20] With its outstanding properties such as excellent photostability, favorable biocompatibility, low toxicity and good water solubility,[21] λex-dependent emission[22] and the up-conversion property,[23] C-dots has emerged into a rising star applied in wide range fields including bioimaging,[24] ion sensors,[25,26] peroxide mimetics,[27] chemiluminescence,[28,29] NO_2 gas sensing,[30] photo-catalysist,[31] antibody carrier,[32] sensitizers for solar cells[33]. For ion sensors, especially mercury ion sensor, several previous reports have tried to apply C-dots for fluorescence detection of Hg^{2+}. For example, Lu et al. explored fluorescence Hg^{2+} probe based on carbon nanoparticles obtained by hydrothermal process of pomelo peel.[18] Using the general concept that adsorption of the fluorescently labeled single-stranded DNA (ssDNA) probe by CNP leads to substantial dye fluorescence quenching and T–Hg^{2+}–T induced hairpin structure does not adsorb on CNP and thus retains the dye fluorescence, Li et al. reported the use of carbon nanoparticles as a fluorescence probe for mercury ions.[34] Elizabeth et al. presented dye-doped polymer nanoparticles that are able to detect mercury ions in aqueous solution at parts per

billion levels via fluorescence resonance energy transfer (FRET).[9] Qin et al. reported on the microwave-assisted rapid synthesis of photoluminescent carbon nanodots exhibiting high sensitivity and selectivity toward Hg^{2+}.[35] Moreover, However, good and promising application performance of carbon dots always involves successive functionalization and surface passivation after synthesis procedure, which is time-consuming and relatively complicated.[19]

Compared with previous hydrothermal method, the proposed method was performed at relatively lower temperature and resulted in larger size (20~30 nm). In the present paper, we completed the syntheses and surface passivation in one step and established a facile and green approach to synthesize a colorimetric and fluoremetric carbon dots probe for the label-free, sensitive, and selective detection of trace mercury ion. Till now, to our best knowledge, there is no related report on any Hg^{2+} probe based on C-dots performing good fluorescent and colorimetric response to Hg^{2+} simultaneously. Polluted water sample analysis shows that trace amount of Hg^{2+} could be detected by both of the colorimetric and fluorescent probes established in the present paper, suggesting promising application of this C-dots in future analysis.

2. Experimental section

2.1. Materials and Apparatus

Citric acid (AR) and ethylenediamine（AR）used to prepared C-dots were

purchased from Sinopharm Chemical Reagent Co., Ltd (China). All chemicals were of analytical grade and used as received without further purification. Hg (□) standard solution series were diluted from standard solution purchased from National Standard Substances Center of China. Doubly distilled water was used throughout the experiments.

Fourier transform infrared (FT-IR) spectrum was performed on an FT-IR spectrophotometer (IR-408PC, BRUKER). Transmission electron microscopy (TEM) measurements of the as-synthesized C-dots was studied on a Tecnai G2 20 electron microscope (FEI， Netherlands). The concentrated C-dots solution was carefully deposited on 400-mesh C-coated Cu grids and excess solvents were evaporated at ambient temperature and pressure. UV/Vis absorbance spectra were obtained on a UV/Vis spectrophotometer (Varian, CA, USA). Fluorescence spectra were recorded by fluorescence spectrophotometer (LS55, PERKINELMER). The X-ray photoelectron spectra (XPS) of Carbon dots were obtained with an X-ray photoelectron spectrometer (GENESIS, EDAX). The samples were prepared by repeatedly spotting the purified Carbon dots solution on titanium slice and allowed to dry in an oven. The binding energies were calibrated with C1s. Quantum yield of the Carbon dots in this paper was measured in accordance with the preceding method.[36] Quinine sulfate in 0.1 mol L-1 H_2SO_4 (literature quantum yield 0.54 at 360 nm) was chosen as a standard while carbon dots was dissolved in distilled water.

2.2. Synthesis of C-dots

C-dots were prepared according to the bottom-up hydrothermal method.[37] Typically, 1.0 g citric acid and 300 μ L ethylenediamine were dissolved in 2 mL water. Then, the solution was transferred to a digestion tube within a digester and heated at 165 ℃ for 150 min. The mixture slowly turned from colorless to a clear brownish solution. After cooled to room temperature, this brownish yellow thick liquid was dialyzed against double distilled water through a dialysis membrane (MWCD=3500). This step went for about 48 hours during which the outside water was changed for several times. Then, the light brown liquid collected after dialysis was stored under 4℃ for further characterization and use.

2.3. Analytical procedure

The detection of Hg^{2+} was performed at room temperature. Typically 1 mL C-dots solution was added into a 10 mL colorimetric tube，followed by the addition of 1 mL 0.1 mol L^{-1} PBS buffer solution (pH 5.0) and a calculated amount of Hg^{2+} ions. The mixed solution was diluted to 10mL with double distilled water. After reaction at room temperature for 15 min, the fluorescence emission spectrums were performed at $\lambda_{ex}/\lambda_{em}$ = 350/448 nm. The absorbance at 302 nm of the reaction solutions above was also recorded. The sensitivity and selectivity measurements were conducted in triplicate.

2.4. Sample pretreatment

Clean tap water samples were collected from tap water system of our laboratory. Polluted tap water sample was collected from the polluted waste water cup in our laboratory. After ultrasonic treatment and filtered through a 0.22 μm membrane, the water sample was used in out test and recovery experiment.

3. Results and discussion

3.1 Characterization

Figure 1

TEM analysis (Figure 1) shows the formation of near spherical but less monodisperse nanoparticles with an average size of 20-30 nm. This size is relatively larger than those reported previously and we assumed this to the lower temperature adopted in present paper. The distance between nanoparticles is markedly short possibly due to the possible hydrogen-bonding interactions among adjacent nanoparticles through the pending hydroxyl end-groups.[38] Based on the experiment results above, we assume that the actual morphology of C-dots in aqueous solution may be small cross-linked molecular clusters and this is consistent with previous study result.[39]

The surface composition and element analysis of the carbon nanodots were conducted by the XPS experiments. As shown in Figure 2a, peaks at 285.6 eV, 401.1eV and 532.8 eV can be ascribed to C1s, N1s and O1s peaks, respectively, indicating carbon nanodots prepared are mainly comprised of C, N and O elements. Content ration of C, N and O is 73.48%, 4.55% and 21.97%. The C1s spectrum (Figure 2b) shows three peaks at 285.6, 287.0, and 289.4 eV, which are attributed to C−C, C-OH/C-NH_2, and O=C-N, respectively. The three peaks at 401.0, 402.5 and 404.7eV in N1s spectrum (Figure 2c) are attributed to N-C=O，N-H and NO_2^- groups, respectively; while the O1s spectrum (Figure 2d) shows four peaks at 530.5, 532.7, 534.2 and 534.3 eV, which are attributed to the C=O, C-O-H, N-O and O-C=O bands, respectively.

Figure 2

FT-IR spectrum of these C-dots (see supporting information Figure S1) shows that the C-dots exhibited characteristic absorption band of O-H stretching vibrations of amine groups at 3359 cm^{-1}, C-H stretching vibration at 2949 cm^{-1}, N–H bending vibrations at 1556 cm^{-1} and C–H bending vibrations at 1186 cm^{-1} and 1076 cm^{-1}. The peaks at 1708 cm^{-1} and 1402 cm^{-1} can be ascribed to the asymmetric and symmetric stretching vibrations of C=O, respectively.[40] The peaks at 775 cm^{-1} can be assigned to the C-H out-of-plane bending mode. [39] In addition to these peaks, we also observe a relatively sharp peak at 1652 cm^{-1} suggestive of amide linkages.

The above observations confirm that the synthesized nanoparticles function with hydroxyl and carboxylic/carbonyl moieties which may originate from raw materials.

Generally speaking, molecular containing rich characteristic groups such as hydroxyl, carboxyl or amine group were excellent candidates of precursor. Citric acid and ethylenediamine, which containing rich carboxyl and amino group respectively, are both typical symbols. We may speculate that C-dots in this paper are mainly prepared by the condensation between citric acid and ethylenediamine and the formation of amino carboxylate. Thus the surface of the C-dots is attached with a lot of pending carboxylate groups, amino groups as well as amino carboxylate group, which can be confirmed by FTIR experiments results. This strategy we assumed above is very similar with the C-dots preparation strategy adopted in the early stage.[41]

3.2 Optical properties of the C-dots

Figure 3

As shown in Figure 3, this C-dots solution shows an absorption band centered at 346 nm and a shoulder peak at 245 nm in the UV/Vis spectrum. Further experiments reveals that upon the addition of Hg^{2+} standard solution, a new absorption peak centered at 302 nm emerges while the weak absorption peak at 346 nm red shifts. Experiment results tell us that red-shift phenomenon above may be ascribed to the strong acid environment brought by the Hg^{2+} standard solution which agreed with previous reports. [39]

Figure 4

For the fluorescence spectrum (Figure 4), the maximum excitation and emission wavelength of C-dots are 350 nm and 448 nm respectively. And as shown in the inset of Figure 4, under a hand-held UV light, strong bright-blue light can be observed from this light brown solution. Similar to various kinds of C-dots reported, we also observe λ_{ex}-dependent fluorescence, suggesting different photoluminescence states existed on the surface of the C-dots. [42] When excited, different photoluminescence states emit their own characteristic emission. The fluorescence quantum yield measured against an aqueous solution of quinine sulfate (λ_{ex} =360 nm) is about 8.9%.

In order to understand C-dots further, we investigate the relationship between its fluorescence and pH. Figure S2 shows the fluorescence curves of C-dots at different pH values. It is obvious that system's fluorescence intensity increases along with the increases of pH value from 2 to 5, but further increase of pH to 10 brings C-dots' fluorescence down. These observations are similar to those of carbon particles modified with hydroxyl and carboxylic. [21,43] In order to improve experiment result, pH 5.0 PBS is used in the following experiments.

Moreover, we investigated the relationship between C-dots' fluorescence intensity and its concentration. The concentration-dependent fluorescence behavior was observed. As shown in Figure S3, fluorescence intensity of C-dots decreased at too high or too low concentration. Self-absorption is often observed in fluorescence materials, including carbon-based materials.[39] This may be ascribed to frequent

collision between particles within C-dots solutions of high concentration. It should be mentioned that fluorescence intensity shows strict linear correlation with concentration in the range from 5.0×10^{-4} mg mL^{-1} to 1.0×10^{-2} mg mL^{-1}(R=0.9996). Considering all these factors, 1.0×10^{-2} mg mL^{-1} C-dots solutions is used in our experiments.

3.3 Colorimetric probe for Hg^{2+}

Figure 5

As shown in Figure 5, the absorption band centered at 302 nm enhances with the addition of increasing amount of Hg^{2+} ions and shows significant linear correlation with the concentration of Hg^{2+}. This phenomenon indicates that as-prepared C-dots could act as a colorimetric probe of Hg^{2+} simultaneously. This colorimetric probe performs well in a wide linear range from 1.0×10^{-9} to 7.0×10^{-7} mol L^{-1} as well as relatively low detection limit of 5.7×10^{-10} mol L^{-1}, which is among the best excellent candidates of Hg^{2+} probe, and is much lower than a previously reported C-dots-based sensing system[44], as well as the maximum allowable level of Hg^{2+} ions in drinking water reported by the US Environmental Protection Agency.[11]

3.4 Selectivity of colorimetric probe towards Hg^{2+}

Figure 6

Specific recognition of the target is particularly important for practical applications of a chemosensor. According previous report, some chemosensors of Hg^{2+} usually interfered with other ions such as Cu^{2+} and Pb^{2+}. The specificity of carbon nanodots towards Hg^{2+} is investigated by measuring absorbance at 302 nm of this colorimetric probe in the presence of 1 equiv. of various metal ions (see in Figure 6). Absorbance at 302 nm is observed at presence of Hg^{2+}, while no similar absorbance observed at presence of other common metal ions. This colorimetric chemosensor shows an excellent specificity towards Hg^{2+} ions.

3.5 Fluorescent probe for Hg^{2+}

Figure 7

As it shown in Figure 4, as-prepared C-dots solution exhibits strong fluorescence emission, which can be quenched by mercury ions effectively. A good linear relationship between the quenching efficiency (F_0/F) and concentration of Hg^{2+} in the range from 7.0×10^{-9} to 7.0×10^{-7} exists, as shown in the inset of Figure 4, where F_0 and F represent fluorescence intensity at 448 nm in the absence and presence of Hg^{2+}, respectively. The linear regression equation is expressed as F_0/F= 2.412+0.452c (c: 10^{-8} mol L^{-1}, n=18) with a correlation efficient of 0.9991. The detection limit is

estimated to be 5.5×10^{-10} mol L^{-1} at a signal-to-noise ratio of 3, which is lower than the upper limit (1.0×10^{-9} mol L^{-1}) of mercury ions content in drinking water permitted by the United States Environmental Protection Agency.[45] And the relative standard deviation is 0.80 % (n=10) for detection of 1.0×10^{-7} mol L^{-1} standard mercury(Ⅱ) ions.

The sensing principle for fluorescence quenching of C-dots by Hg^{2+} is presumably due to facilitating nonradiative electron/hole recombination annihilation through an effective electron or energy transfer process.[44,46]

3.6 Selectivity of fluorescence probe towards Hg^{2+}

Figure 8

Figure 8 depicts the fluorescence response of C-dots to various metal cations and its selectivity for Hg^{2+}. The experiment results suggest that the fluorescence intensity of this noble sensing probe is hardly affected (below 1 %) by a background of environmentally relevant alkali or alkali earth metal ions and transition metal cations (each with a concentration of 5 equiv.). It should be mentioned that this C-dots shows good selectivity for Hg^{2+} over Cu^{2+} and Pb^{2+}, because Cu^{2+} and Pb^{2+} ions usually are the interfering components for the mercury ion detection.[47] Furthermore, the selectivity of C-dots against a more complex background containing another one competing ion and Hg^{2+} is evaluated considering of cross reactivity. As shown in

Figure 8, obviously, this C-dots probe still made excellent performance at presence of other interfering ions. This prominent selectivity may be ascribed to that Hg^{2+} has a stronger affinity towards the rich carboxylic group on the surface of C-dots than other metal ions.[48]

3.7 Stability of system

The stability of system was investigated by observing the fluorescence intensity of the solutions in the absence and presence of Hg^{2+} (7.0×10^{-7} mol L^{-1}) in a period of 1 hour. As shown in Figure S4, the fluorescence of C-dots and the quenched fluorescence maintained stable in following one hour. In fact, the C-dots stock solution stored at 4 ℃ for more than two months still give bright fluorescence, which may be attributed to their small particle size and electrostatic repulsions between them.[18] The result indicates that this quenching method is a rapid and stable for the detection of Hg^{2+} ions.

3.8 Comparison of methods

Table 1

The comparison of C-dots with other reagents for mercury detection is shown in Table 1. It can be seen in Table 1 that fluorometric and colorimetric probe for mercury

ion based on C-dots is comparable with or more selective than those reported before in sensibility. The proposed method is relatively simple, rapid, selective and sensitive for determination of mercury ions.

3.9 Sample analysis

Table 2

The practical applicability of the two sensing methods established in this paper is evaluated through detecting content of Hg^{2+} in polluted tap water sample and comparing results obtained with standard experiment (AAS). The results are shown in Table 2 and table 3. The concentrations of Hg^{2+} in two parallel samples determined using the proposed method are basically consistent with the results measured by atomic absorption spectrometry (AAS).

Table 3

This water samples were spiked with standard solutions containing three different concentration levels of mercury ions then analyzed with our two methods. As shown in Table 4 and Table 5, in spite of interference from numerous minerals existing in tap water, the results show good agreement with the added and found value. The recovery rate acquired is between 99.8-101.2%, showing a promising application of Hg^{2+} detection.

Table 4

Table 5

4. Conclusions

In summary, a new colorimetric and fluorescence probe for Hg^{2+} ions detection is developed based on a one-step hydrothermal method synthesized C-dots. Compared with previous hydrothermal method, the proposed method was performed at relatively lower temperature and resulted in larger size (20~30 nm). No further chemical modification of C-dots is required, which offers the advantages of simplicity and cost efficiency. Both of the colorimetric and fluorescence probe shows excellent sensitivity and good selectivity over other transition metal ions for Hg^{2+} ions detection with detection limits of 5.7×10^{-10} mol L^{-1} and 5.5×10^{-10} mol L^{-1}, respectively. And they have also been successfully applied to the analysis of polluted tap water sample and we believe its simplicity, sensitivity and specificity will make it promising for monitoring mercury pollution in the environment.

Acknowledgment

This project was financially supported by the National Natural Science Foundation of

China (20805016).

Appendix A. Supplementary data

Reference

[1] A. Renzoni, F. Zino and E. Franchi, *EnViron. Res.*, 1998, 77, 68-72.

[2] O. Malm, *EnViron. Res.*, 1998, 77, 73-78.

[3] P. B. Tchounwou, W. K. Ayensu, N. Ninashvili and D. Sutton, *Environ. Toxicol.*, 2003, 18, 149-175.

[4] E. Nolan, S. Lippard, *Chem. Rev.*, 2008, 108, 3433-3480.

[5] Y. F. Zhang, Q. Yuan, T. Chen, X. B. Zhang, Y. Chen and W. H. Tan, *Anal. Chem.*, 2012, 84, 1956-1962.

[6] Y. Q. Chen, H. Bai, W. J. Hong and G. Q. Shi, *Analyst*, 2009, 134, 2081-2086.

[7] H. N. Kim, W. X. Ren, J. S. Kim and J. Yoon, *Chem. Soc. Rev.*, 2012, 41, 3210-3244.

[8] S. Hazra, S. Balaji, M. Banerjee, A. Ganguly, N. N. Ghosh and A. Chatterjee, *Anal. Methods*, 2014, 6, 3784-3790.

[9] E. S. Childress, C. A. Roberts, D. Y. Sherwood, C. L. M. LeGuyader and E. J. Harbron, *Anal. Chem.*, 2012, 84, 1235-1239.

[10] C. C. Huang, Z. S. Yang, K. H. Lee and H. T. Chang, *Angew. Chem. Int. Ed.*, 2007, 46, 6824-6828.

[11] W. W. Guo, J. P. Yuan and E. K. Wang, *Chem. Commun.*, 2009, 23, 3395--3397.

[12] S. L. Li, H. Deng, W. P. Cao, C. Q. Zhang, S. B. Jin, X. D. Xue, J. C. Zhang, G. Z. Li and X. J. Liang, *Analyst*, 2014, 139, 3369-3372.

[13] L. B. Zhang, T. Li, B. B. Li, J. Li and E. K. Wang, *Chem. Commun.*, 2010, 46, 1476-1478.

[14] L. Q. Guo, N. Yin, D. D. Nie, J. R. Gan, M. J. Li, F. F. Fu and G. N. Chen, *Analyst*, 2011, 136, 1632-1636.

[15] C. H. Li and S. Y. Liu, *J. Mater. Chem.*, 2010, 20, 10716-10723.

[16] J. P. Xu, Z. G. Song, Y. Fang, J. Mei, L. Jia, A. J. Qin, J. Z. Sun, J. Ji and B. Z. Tang, Analyst, 2010, 135, 3002-3007.

[17]H. L. Li, J. F. Zhai and X. P. Sun, Nanoscale, 2011, 3, 2155-2157.

[18] W. B. Lu, X. Y. Qin, S. Liu, G. H. Chang, Y. W. Zhang, Y. L. Luo, M. A. Abdullah, A. Abdulrahman O and X. P. Sun, *Anal. Chem.*, 2012, 84, 5351-5357.

[19] Y. L. Ma, Y. Sheng, C. Q. Tang, X. H. Hong, S. C. Chen, D. Q. Zhu and Q. D. Zheng, *Sensors and Actuators B*, 2013, 176, 132-140.

[20] Y. B. Song, S. J. Zhu and B. Yang, *RSC Adv.*, 2014, 4, 27184-27200.

[21] H. P. Liu, T. Ye and C. D. Mao, *Angew. Chem. Int. Ed.*, 2007, 46, 6473-6475.

[22] Y. P. Sun, B. Zhou, Y. Lin, W. Wang, K. A. S. Fernando, P. Pathak, M. J. Meziani, B. A. Harruff, X. Wang, H. F. Wang, P. J. G. Luo, H. Yang, M. E. Kose, B. L. Chen, L. M. Veca and S. Y. Xie, *J. Am. Chem. Soc.*, 2006, 128, 7756-7757.

[23] H. Zhang, H. Huang, H. Ming, H. Li, L. Zhang, Y. Liu and Z. J. Kang, *Mater. Chem.*, 2012, 22, 10501-10506.

[24] L. Cao, X. Wang, M. J. Meziani, F. S. Lu, H. F. Wang, P. J. G. Luo, Y. Lin, B. A. Harruff, L. M. Veca, D. Murray, S. Y. Xie and Y. P. Sun, *J. Am. Chem. Soc.*, 2007, 129, 11318-11319.

[25] Y. Q. Dong, R. X. Wang, G. L. Li, C. Q. Chen, Y. W. Chi and G. N. Chen, *Anal. Chem.*, 2012, 84, 6220-6224.

[26] Q. Wang, X. Liu, L. C. Zhang and Y. Lv, *Analyst*, 2012, 137, 5392-5397.

[27] W. B. Shi, Q. L. Wang, Y. J. Long, Z. L. Cheng, S. H. Chen, H. Z. Zheng and Y. M. Huang, *Chem. Comm.*, 2011, 47, 6695-6697.

[28] J. X. Shi, C. Lu, D. Yan and L. Ma, *Biosensors and Bioelectronics*, 2013, 45, 58-64.

[29] Y. Zhou, G. W. Xing, H. Chen, N. Ogawa and J. M. Lin, *Talanta*, 2012, 99, 471-477.

[30] R. X. Wang, G. L. Li, Y. Q. Dong, Y. W. Chi and G. N. Chen, *Anal. Chem.*, 2013, 85, 8065-8069.

[31] H. T. Li, R. H. Liu, S. Y. Lian, Y. Liu, H. Huang and Z. H. Kang, *Nanoscale*, 2013, 5, 3289-3297.

[32] H. Dai, C. P. Yang, Y. J. Tong, G. F. Xu, X. L. Ma, Y. Y. Lin and G. N. Chen, *Chem. Commun.*, 2012, 48, 3055-3057.

[33] P. Mirtchev, E. J. Henderson, N. Soheilnia, C. M. Yipc and G. A. Ozin, *J. Mater. Chem.*, 2012, 22, 1265-1269.

[34] H. L. Li, J. F. Zhai, J. Q. Tian, Y. L. Luo and X. P. Sun, *Biosens, and Bioelectro.* 2011, 26, 4656-4660.

[35] X. Y. Qin, W. B. Lu, A. M. Asiri, A. O. Al-Youbi and X. P. Sun, *Sensors and Actuators B*, 2013, 184, 156-162.

[36] J. R. Lakowicz, Principles of Fluorescence Spectroscopy, second ed., Kluwer Academic/Plenum Publishers, New York, 1996.

[37] S. J. Zhu, Q. N. Meng, L. Wang, J. H. Zhang, Y. B. Song, H. Jin, K. Zhang, H. C. Sun, H. Y. Wang and B. Yang, *Angew. Chem. Int. Ed.*, 2013, 52, 3953-3957.

[38] A. B. Bourlinos, A. Stassinopoulos, D. Anglos, R. Zboril, M. Karakassides and E. P. Giannelis, *Small*, 2008, 4, 455-458.

[39] Y. B. Song, S. J. Zhu, S. Y. Xiang, X. H. Zhao, J. H. Zhang, H. Zhang, Y. Fu and

B. Yang, *Nanoscale*, 2014, 6, 4676-4682.

[40] M. J. Bojdys, J. O. Muller, M. Antonietti and A. Thomas, *Chem.Eur. J.*, 2008, 14, 8177-8182

[41] C. J. Jiang, D. J. Cardin and S. C. Tsang, *Chem. Mater.*, 2008, 20, 14-16.

[42] S. Zhu, J. Zhang, S. Tang, C. Qiao, L. Wang, H. Wang, X. liu, B. Li, Y. Li, W. Yu, X. Wang, H. Sun and B. Yang, *Adv. Funct. Mater.*, 2012, 22, 4732-4740.

[43] Q. Zhao, Z. Zhang, B. Huang, J. Peng, M. Zhang and D. Pang, *Chem. Commun.*, 2008, 41, 5116-5118.

[44] L. Zhou, Y. Lin, Z. Huang, J. Ren and X. Qu, *Chem.Commun.*, 2012, 48, 1147-1149.

[45] Y. Gong, X. Zhang, Z. Chen, Y. Yuan, Z. Jin, L. Mei, J. Zhang, W. Tan, G. Shen and R. Yu, *Analyst*, 2012, 137, 932-938.

[46] Y. Xia and C. Zhu, *Talanta*, 2008, 75, 215-221.

[47] R. Kramer, *Angew. Chem.*, 1998, 37, 772-773.

[48] F. Chai, C. Wang, T. Wang, Z. Ma and Z. Su, *Nanotechnology*, 2010, 21, 25501-25506.

Tables:

Table 1 Comparison of methods

Reagent	Performance		Method	Ref
	Linear range(mol L^{-1})	LOD(mol L^{-1})		
Polymer nanoparticles	3.5×10^{-9}~5.0×10^{-8}	3.5×10^{-9}	Ratiomatric	[9]
AuNPs	1.0×10^{-9}~1.0×10^{-3}	1.0×10^{-9}	Fluorescence recovery	[10]
Ag nanoclusters	5.0×10^{-9}~1.0×10^{-7}	5.0×10^{-9}	Fluorescence quenching	[11]
CWQ-11/T_{33}*	1.0×10^{-7}~1.0×10^{-6}	3.0×10^{-7}	Fluorescence recovery	[12]
Carbon nanotube–DNA hybrid	5.0×10^{-8}~8.0×10^{-6}	1.45×10^{-8}	Fluorescence recovery	[13]
Carbon-nanotubes	2.0×10^{-8}~1.25×10^{-6}	7.9×10^{-9}	Fluorescence recovery	[14]
PIFPC	1.0×10^{-7}~1.0×10^{-6}	7.4×10^{-7}	Fluorescence quenching	[19]
C-dots	7.0×10^{-9}~7.0×10^{-7}	5.5×10^{-10}	Fluorescence quenching	This work
C-dots	1.0×10^{-9}~7.0×10^{-7}	5.7×10^{-10}	Colorimetric	This work

*T_{33} means ssDNA containing 33 T residues while CWQ-11 means carbazole-based cyanine.

Table 2 Results of Hg^{2+}detection in polluted tap water sample by colorimetric probe

Sample	Content（$\times 10^{-8}$ mol L^{-1}）		Er(%)
	AAS	Colorimetric	
1	6.3	5.9	-6.3
2	37.7	39.0	3.4

Table 3 Recovery of tap water sample experiment adapting colorimetric method

	Added Hg^{2+}/nM	Found mean[a]±SD[b]/nM	Recovery/%
Tap water 1	5.00	5.06±0.18	101.2
Tap water 2	50.0	50.5±1.1	101.0
Tap water 3	500	502±18.0	100.4

[a] Mean of three determinations; [b] standard deviation

Table 4 Results of Hg^{2+}detection in polluted tap water sample by fluorescent probe

Sample	Content（$\times 10^{-8}$ mol L^{-1}）		Er(%)
	AAS	Fluorescent	
1	6.3	5.7	-9.5
2	37.7	38.9	3.2

Table 5 Recovery of tap water sample experiment adapting fluorescence method

	Added Hg^{2+}/nM	Found mean[a]±SD[b]/nM	Recovery/%
Tap water 1	5.00	5.01±0.04	100.2
Tap water 2	50.0	49.9±0.1	99.8
Tap water 3	500	501±15.5	100.2

[a] Mean of three determinations; [b] standard deviation

Figure captions:

Figure 1 Typical transmission electron microscopy (TEM) image (Figure 1a) of the as-prepared C-dots. The corresponding nanoparticle size distribution histogram obtained by counting about 80 particles (Figure 1b) indicates that diameters of these C-dots dispersed in the solution ranges from 10-40nm.

Figure 2 (a) XPS; (b) C1s; (c) N1s; (d) O1s spectra of as-prepared carbon nanodots.

Figure 3 UV-Vis absorption spectra of the aqueous solution of as-prepared C-dots. (1: UV-Vis absorbance of C-dots solution; 2-4: after adding certain amount of Hg^{2+} ions)

Figure 4 Fluorescence spectra of C-dots at different excitation wavelengths. Inset: the photograph of C-dots solution under UV light (365 nm) (left) and daylight (right).

Figure 5 Absorbance responses of C-dots upon the addition of different concentration Hg^{2+} solution (PBS pH 5.0) from 0 to 7.0×10^{-7} mol L^{-1}. The inset is linear relationship between the absorbance and Hg^{2+} concentration over the range of 1.0×10^{-9}~7.0×10^{-7} mol L^{-1}. The error bars represent standard deviations based on three independent measurements.

Figure 6 Selectivity of colorimetric sensing of the C-dots for Hg^{2+}. Blank means the C-dots solution without any metal ions. Experiment condition: carbon dots: 1×10^{-2} mg mL^{-1}; PBS: 0.1mol L^{-1}, pH=5.0; Hg^{2+}:5.0×10^{-7}; interfering ions: 5.0×10^{-7} mol L^{-1}.

Figure 7 Fluorescence response of 0.01mg mL^{-1} C-dots at presence of increasing concentrations of Hg^{2+} (from top to bottom, 0, 7.0×10^{-9}, 8.0×10^{-9}… … 7.0×10^{-7} mol L^{-1} in PBS (pH 5.0). The inset is Stern-Volmer plot showing the linear relationship between the fluorescence intensity and Hg^{2+} concentration over the range of 7.0×10^{-9}-7.0×10^{-7} mol L^{-1}. The error bars represent standard deviations based on three independent measurements.

Figure 8 Selectivity of the C-dots for Hg^{2+}. Blank means the C-dots solution without any metal ions. F_0 means the fluorescence of blank C-dots solution without any metal ions, while F represents the fluorescence at presence of different metal ions. F_0/F could indicate the quenching degree of different metal ions. The blue bars represent the quenching degree of different single metal ion while the red bars stand for the quenching state within solutions at presence of both Hg^{2+} and another competing ion. The concentration of Hg^{2+} is 5.0×10^{-7} mol L^{-1}, and K^{+} and Al^{3+} are used in a concentration of 5 equivalents, while other metal ions used are 5.0×10^{-7} mol L^{-1}.

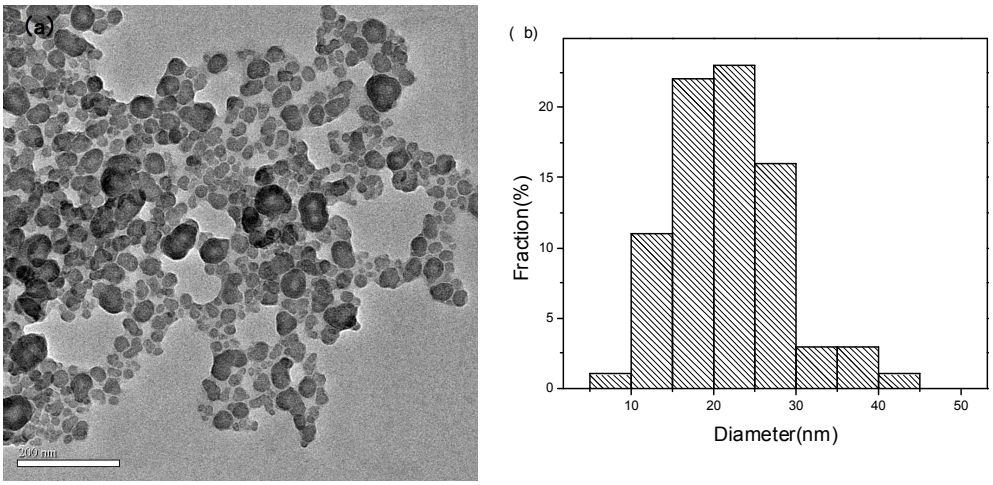

Figure 1

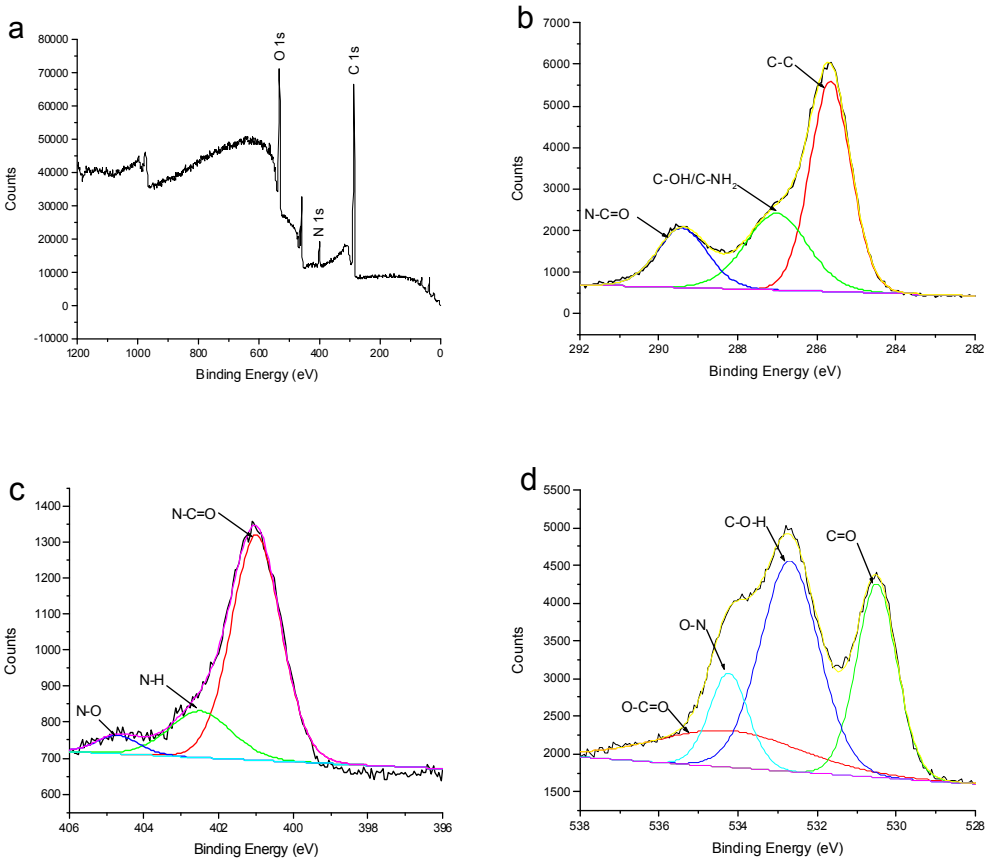

Figure 2

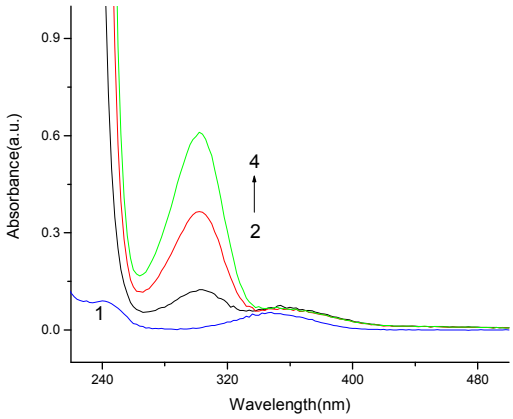

Figure 3

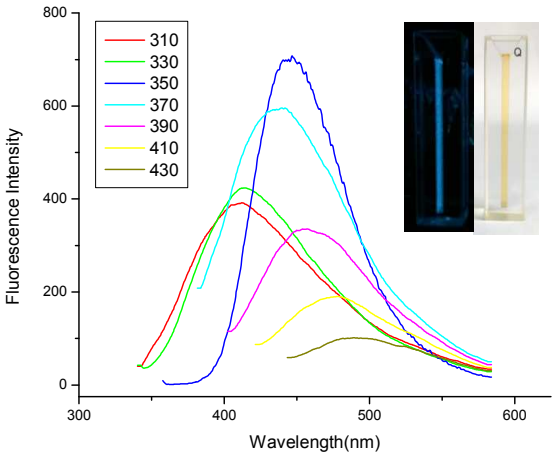

Figure 4

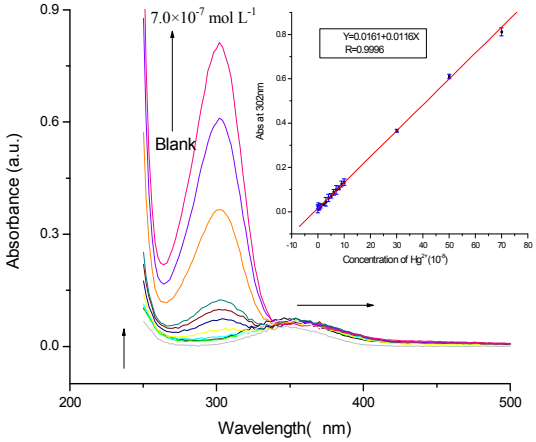

Figure 5

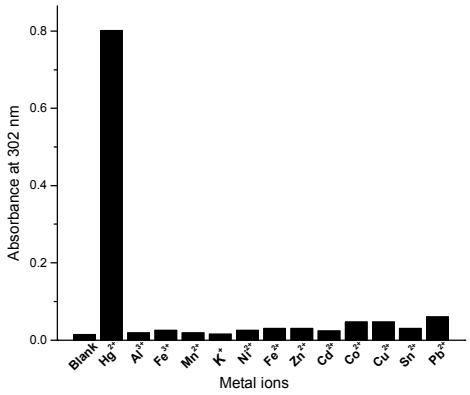

Figure 6

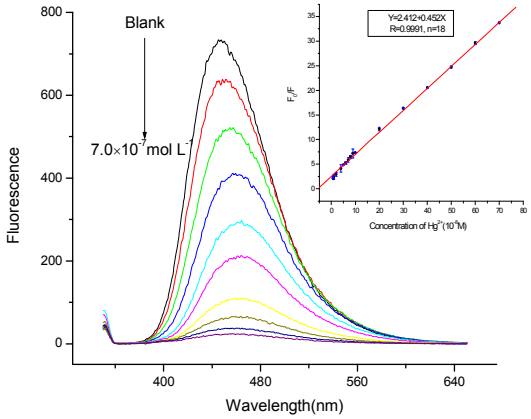

Figure 7

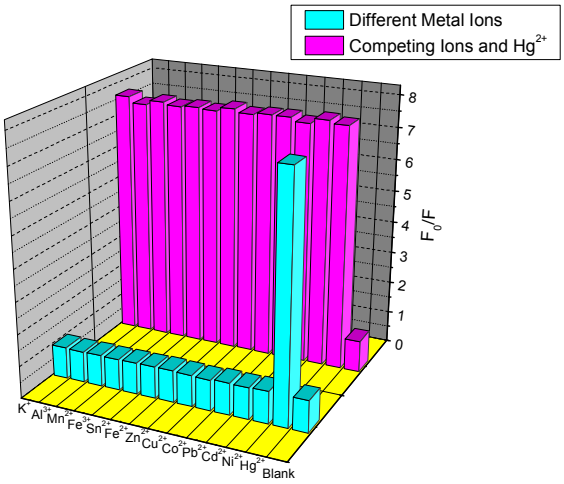

Figure 8